AIChE

Covariance-Based Hardware Selection-Part III: Distributed Parameter Systems

Syed K. Ahmed, Jui-Kun Peng, and Donald J. Chmielewski
Dept. of Chemical and Biological Engineering, Illinois Institute of Technology, Chicago, IL 60616

DOI 10.1002/aic.12782
Published online November 2, 2011 in Wiley Online Library (wileyonlinelibrary.com).

In this article, we propose a new method for the selection of control system hardware (sensors and actuators) for distributed parameter systems. The proposed design scheme seeks to minimize the capital cost of hardware while satisfying predefined performance constraints. Within this minimum capital cost framework, three design scenarios will be discussed; the closed-loop full state information actuator selection problem, the open-loop partial state information sensor selection problem, and the closed-loop partial state information simultaneous sensor and actuator selection problem. The proposed method will be illustrated through application to a nonisothermal tubular reactor example. © 2011 American Institute of Chemical Engineers *AIChE J,* 58: 2705–2713, 2012

Keywords: sensor selection, actuator selection, process control, optimization, linear matrix inequalities, mixed integer convex programming

Introduction

The appropriate selection of hardware (sensors and actuators) will have a dominating impact on control system performance. That is, the quality of information gathered along with the ability to influence the process is likely more important than the control algorithm used for regulation, assuming a reasonably designed regulator. As such, an enormous body of literature exists on the subject of hardware selection. Early efforts focused exclusively on sensor selection by defining a quantitative measure for information quality. For example, Johnson[1] and Muller and Weber[2] both focused on selecting a sensor array to maximize the observability of a finite-dimensional dynamic process. Additional hardware selection efforts aimed at finite-dimensional dynamic systems include Mellefont and Sargent,[3] Morari and Stephanopoulos,[4] Romagnoli et al.,[5] Bagajewicz,[6] Chmielewski et al.,[7] Muske and Georgakis,[8] Alonso et al.,[9] Singh and Hahn,[10] and Peng and Chmielewski.[11,12] The topic of control structure selection could also be considered a hardware selection effort. A small sampling of this literature includes Morari et al.,[13] Hovd and Skogestad,[14] Narraway and Perkins,[15] Lee et al.,[16] Loeblein and Perkins,[17] Cao and Rossiter,[18] Wisnewski and Doyle,[19] Heath et al.,[20] and van de Wal and de Jager.[21] Many of the hardware selection efforts focus on distributed parameter (or infinite-dimensional) dynamic systems. A sampling of these efforts include Yu and Seinfeld,[22] Kumar and Seinfeld,[23] Harris et al.,[24] Morari and O'Dowd,[25] Van de Wouwer et al.,[26] Faulds and King,[27] Antoniades and Christofides,[28] and Armaou and Demetriou.[29] In the survey paper by Kubrusly and Malebranche,[30] the infinite-dimensional methods are classified as early or late lumping to denote when the spatial discretization step occurs within the procedure. In the late lumping cases, the infinite-dimensional representation is retained throughout the design phase, and discritization is used in the last step to arrive at a finite-dimensional controller. The current effort would be classified as an early lumping procedure, as it begins with a spatial discretization step to arrive at a finite-dimensional approximation of the process, from which a finite controller is designed for candidate hardware configurations.

In the following section, a method is illustrated for conversion of a distributed parameter model into a form suitable for the proposed hardware selection approach. Then, the hardware selection optimization problems of Peng and Chmielewski[12] are adapted to the new model structure. Given this hardware selection context, the tubular reactor example is developed in detail. Then, the important step of augmenting the process model with actuator dynamics and an appropriate disturbance model is illustrated. Finally, a set of tubular reactor case studies is presented to illustrate the parametric data needed, the types of solutions one should expect, and the computational effort required.

System Modeling

Consider the following partial differential equation (PDE) description of a generic distributed parameter system.

$$\frac{\partial \xi}{\partial t} = \mathcal{L}_s \xi + \mathcal{A}(s)\xi + \mathcal{B}(s)\mu + \mathcal{G}(s)\omega \tag{1}$$

where $s \in [0, 1]$ and $t \in [0, \infty)$ are the spatial and temporal coordinates, respectively, $\mathcal{L}_s$ is a linear differential operator with respect to s, $\xi(s, t)$ is the infinite-dimensional state, $\mu(s, t)$

Correspondence concerning this article should be addressed to D. J. Chmielewski at chmielewski@iit.edu.
Current Address of Jui-Kun Peng: Nuclear Engineering Division, Argonne National Laboratory, Argonne, IL 60439.

is the manipulated input, and $\omega(s, t)$ is the disturbance. In this section, and without loss of generality, we assume $\xi(s, t)$ is a scalar function with boundary conditions of the form

$$\mathcal{M}_{s,i}\xi(s_i^{(\mathrm{b})}, t) = \xi_i,\ i = 1 \ldots n_{\mathrm{b}} \quad \text{for all } t \tag{2}$$

where $\mathcal{M}_{s,i}$ are differential operators and $s_i^{(b)}$ are the condition locations. Next assume the inputs take a finite-dimensional decomposable form and can be represented as

$$\mu(s,t) = \sum_{i=1}^{n_u} g_i^{(u)}(s)u_i(t) \tag{3}$$

$$\omega(s,t) = \sum_{i=1}^{n_w} g_i^{(w)}(s)w_i(t) \tag{4}$$

This class includes the point-wise form; $g_i^{(k)}(s) = \delta\ (s - s_i^{(k)})$ where $\delta(s)$ is the Dirac delta function and $s_i^{(k)}$ is the input location, $k = u$ or w.

Regarding measurements, again assume a finite-dimensional decomposable form

$$\theta_i(t) = \int_0^1 g_i^{(y)}(s)\xi(s,t)ds + v_i(t) \quad i = 1, \ldots, n_y \tag{5}$$

where θ_i is a scalar measurement signal and v_i is the noise associated with sensor i. This class also includes a point-wise form; $g_i^{(y)}(s) = \delta\ (s - s_i^{(y)})$ where $s_i^{(y)}$ is the measurement location, which simplifies Eq. 5 to $\theta_i(t) = \xi\ (s_i^{(y)}, t) + v_i(t)$. It will also be convenient to define a set of performance signals $\zeta_i(t)$. These have a form similar to that of the measurements

$$\zeta_i(t) = \int_0^1 g_i^{(z)}(s)\xi(s,t)ds \quad i = 1, \ldots, n_z \tag{6}$$

In the sequel, the definition $\theta(t) = [\,\theta_1(t)\ \ \theta_2(t)\ \ \ldots\ \ \theta_{n_y}(t)\,]^T$ and $\zeta(t) = [\,\zeta_1(t)\ \ \zeta_2(t)\ \ \ldots\ \ \zeta_{n_z}(t)\,]^T$ will be utilized.

Assume $\xi(s, t)$ is spanned by a series of trial function $\rho_i(s)$ and, thus, may be expressed in the following form

$$\xi(s,t) = \sum_{i=1}^{\infty} \rho_i(s)x_i(t) \tag{7}$$

The functions $\rho_i(s)$ can be selected as the eigenfunctions of $\mathcal{L}_s$ or may be any complete set on the interval [0, 1]. Without loss of generality, we assume that each $\rho_i(s)$ satisfies the boundary conditions of Eq. 2. To obtain a finite-dimensional representation of $\xi(s, t)$, define $\xi^{(N)}(s, t)$

$$\xi(s,t) \approx \xi^{(N)}(s,t) = \sum_{i=1}^{N} \rho_i(s)x_i(t) \tag{8}$$

Following the standard Galerkin approach,[31–33] we evaluate $\langle \rho_i, R_N \rangle = 0$ for $i = 1,\ldots,N$ where the inner product $\langle \rho_i, \rho_j \rangle$ is defined as $\int_0^1 \varphi(s)\rho_i(s)\rho_j(s)ds$, $\varphi(s)$ is an appropriate weighting function and R_N is the residual function defined as: $R_N(s,t) = \frac{\partial \xi^{(N)}}{\partial t} - \mathcal{L}_s\xi^{(N)} - \mathcal{A}(s)\xi^{(N)} - \mathcal{B}(s)\mu - \mathcal{G}(s)\omega$. Following the algebra through, one arrives at the following finite dimensional description

$$\frac{dx}{dt} = Ax + Bu + Gw \tag{9}$$

where $x = [x_1(t)\ x_2(t), \ldots, x_N(t)]^T$, $u = [u_1(t)u_2(t), \ldots, u_{n_u}(t)]^T$, $w = [w_1(t)w_2(t), \ldots, w_{n_w}(t)]^T$, $A = M^{-1}\overline{A}$, $B = M^{-1}\overline{B}$, and $G = M^{-1}\overline{G}$. The elements of M, $\overline{A}$, $\overline{B}$, and $\overline{G}$ are $m_{ij} = \langle \rho_i, \rho_j \rangle$ (i is the row and j is the column throughout), $\bar{a}_{ij} = \langle \rho_j, (\mathcal{L}_s + \mathcal{A})\rho_i \rangle$, $\bar{b}_{ij} = \langle \rho_j, \mathcal{B}g_i^{(u)} \rangle$, and $\bar{g}_{ij} = \langle \rho_j, \mathcal{G}g_i^{(\omega)} \rangle$. If $\rho_i(s)$ are orthonormal eigenfunctions of $\mathcal{L}_s$ (i.e., $\mathcal{L}_s\rho_i(s) = \lambda_i\rho_i(s)$ and $\varphi(s)$ is defined such that $\langle \rho_i, \rho_j \rangle = \delta_{ij}$, where δ_{ij} is the Kronecker delta function), then M will be the identity matrix and $\bar{a}_{ij} = \lambda_i\delta_{ij} + \langle \rho_i, \mathcal{A}\rho_j \rangle$. If the system has pointwise inputs, then $\bar{b}_{ij} = \varphi(s_j^{(u)})\rho_i(s_j^{(u)})\mathcal{B}(s_j^{(u)})$ and $\bar{g}_{ij} = \varphi(s_j^{(w)}) \times \rho_i(s_j^{(w)})\mathcal{G}(s_j^{(w)})$. Returning to the measurement and performance outputs, one finds

$$\theta \approx y = Cx + v \tag{10}$$

$$\zeta \approx z = Dx \tag{11}$$

where $y = [y_1(t)y_2(t),\ldots,y_{ny}(t)]^T$ and v and z are similarly defined. The elements of C and D are $c_{ij} = \int_0^1 g_i^{(y)}(s)\rho_j(s)ds$ and $d_{ij} = \int_0^1 g_i^{(z)}(s)\rho_j(s)ds$. If the outputs have a point-wise form then, $c_{ij} = \rho_j(s_i^{(y)})$ and $d_{ij} = \rho_j(s_i^{(z)})$. It is important to note that the multitude of integrals required to determine the matrices A, B, G, C, and D need only be performed once for a given set of trial functions $\rho_i(s)$ and desired accuracy N.

Covariance Analysis and Hardware Selection

Given the above system description, it is a simple matter to apply steady-state covariance analysis. Start with the open-loop system (i.e., $u(t) = 0$ for all t), and let w be a Gaussian zero mean, white process with spectral density S_w. Then the steady-state covariance of x is $\Sigma_x \geq 0$ such that $A\Sigma_x + \Sigma_x A^T + GS_wG^T = 0$. The steady-state covariance of z is $\Sigma_z = D\Sigma_x D^T$. Next, define ϕ_i as the ith row of an appropriately sized identity matrix to determine the steady-state variance of the scalar signal $z_i(t)$ as $\sigma_{zi}^2 = \phi_i D\Sigma_x D^T\phi_i^T$.

In the closed-loop full state information (FSI) case $u(t) = Lx(t)$, where L should be selected such that $(A + BL)$ is stable. In this case, the steady-state covariance of $z_i(t)$ is $\sigma_{zi}^2 = \phi_i D\Sigma_x D^T\phi_i^T$, where $\Sigma_x \geq 0$ satisfies $(A + BL)\Sigma_x + \Sigma_x(A + BL)^T + GS_wG^T = 0$. Also the steady-state variance of $u_i(t)$ is given by $\sigma_{ui}^2 = \phi_i L\Sigma_x L^T\phi_i^T$. As in Chmielewski and Peng[34], the attendance of an actuator is indicated by the performance bound $\phi_i L\Sigma_x L^T\phi_i^T < \alpha_i\bar{u}_i^2$, where $\alpha_i = 0$ or 1 indicates the absence or presence of actuator i, respectively, and $\bar{u}_i$ is largest standard deviation allowed for actuator i. Then, given actuator costs, $c_i^{(u)}$, and a set of performance bounds on the output signals, $\sigma_{z_i}^2 < \bar{z}_i^2$, $i = 1 \ldots n_z$, one may formulate the following FSI actuator selection problem.

$$\begin{aligned} \min_{\alpha_i \in \{0,1\}, \Sigma_x \geq 0, L} \quad & \sum_{i=1}^{n_u} c_i^{(u)}\alpha_i \\ s.t. \quad & \phi_i D\Sigma_x D^T\phi_j^T < \bar{z}_i^2, \quad i = 1, \ldots, n_z \\ & \phi_i L\Sigma_x L^T\phi_i^T < \alpha_i\bar{u}_i^2, \quad i = 1, \ldots, n_u \\ & (A + BL)\Sigma_x + \Sigma_x(A + BL)^T + GS_wG^T = 0 \end{aligned} \tag{12}$$

The mixed integer nonlinear program (MINLP) of Eq. 12 can be converted to the following computationally attractive form of a mixed integer convex program (MICP) (see Chmielewski and Peng[34] for details).

$$\min_{\alpha_i\in\{0,1\},X>0,Y} \quad \sum_{i=1}^{n_u} c_i^{(u)}\alpha_i$$
$$\text{s.t.} \quad \phi_i DXD^T\phi_i^T < \bar{z}_i^2, \quad i=1,\ldots,n_z$$
$$\begin{bmatrix} \alpha_i\bar{u}_i^2 & \phi_i Y \\ Y^T\phi_i^T & X \end{bmatrix} > 0, \quad i=1,\ldots,n_u$$
$$(AX+BY)+(AX+BY)^T + GS_wG^T < 0 \qquad (13)$$

If α_i*, X*, and Y* denote the solution to Eq. 13, then a feasible controller under the actuator configuration α_i* can be obtained as $L = Y^*(X^*)^{-1}$.

In the open-loop partial state information (PSI) case, the measurement signal, $y = Cx + v$, is used to construct an estimate, $\hat{z}$, of the performance output z. If w and v are Gaussian zero mean, white processes with spectral densities S_w and S_v, then the optimal estimate of z is $\hat{z} = D\hat{x}$ where $\hat{x}$ is generated by the state estimator

$$\dot{\hat{x}} = A\hat{x} + Bu + \Sigma_e C^T\Sigma_v^{-1}(y - C\hat{x}) \qquad (14)$$

where $\Sigma_e \geq 0$ satisfies

$$A\Sigma_e + \Sigma_e A^T + GS_wG^T - \Sigma_e C^T S_v^{-1} C\Sigma_e = 0 \qquad (15)$$

Recalling that Σ_e is the steady-state covariance of the error signal $e(t) = x(t) - \hat{x}(t)$, one finds that the steady-state variance of the error output signal, $e_{zi} = z_i - \hat{z}_i$, is $\sigma_{ezi}^2 = \phi_i D\Sigma_e D^T\phi_i^T$. As in Peng and Chmielewski,[12] the attendance of sensors is indicated by the matrix $S_v^{-1} = \text{diag}\{\beta_i/\bar{\sigma}_{v_i}^2\}$ where $\bar{\sigma}_{v_i}^2$ is the noise spectral density associated with sensor i and $\beta_i = 0$ or 1 indicates the absence or presence of sensor i, respectively. Then given sensor costs, $c_i^{(y)}$, along with a set of error variance performance bounds $\sigma_{e_{zi}}^2 < \bar{e}_{zi}^2$, $i = 1\ldots n_z$, one can formulate the open-loop sensor selection problem as follows

$$\min_{\beta_i\in\{0,1\},\Sigma_e\geq 0} \quad \sum_{i=1}^{n_y} c_i^{(y)}\beta_i$$
$$s.t. \quad \phi_i D\Sigma_e D^T\phi_i^T < \bar{e}_{zi}^2, i=1,\ldots,n_z$$
$$A\Sigma_e + \Sigma_e A^T + GS_wG^T - \Sigma_e C^T S_v^{-1} C\Sigma_e = 0$$
$$S_v^{-1} = \text{diag}\{\beta_i/\bar{\sigma}_{v_i}^2\} \qquad (16)$$

The MINLP of Eq. 16 can be converted to the following MICP (see Peng and Chmielewski[12] for details)

$$\min_{\beta_i\in\{0,1\},W>0} \quad \sum_{i=1}^{n_y} c_i^{(y)}\beta_i$$
$$s.t. \quad \begin{bmatrix} \bar{e}_{zi}^2 & \phi_i D \\ D^T\phi_i^T & W \end{bmatrix} > 0, \quad i=1,\ldots,n_z$$
$$\begin{bmatrix} C^T S_v^{-1} C - A^T W - WA & WG \\ G^T W & S_w^{-1} \end{bmatrix} > 0$$
$$S_v^{-1} = \text{diag}\{\beta_i/\bar{\sigma}_{v_i}^2\} \qquad (17)$$

In the closed-loop PSI case, $u(t) = L\hat{x}(t)$, $\sigma_{z_i}^2 = \phi_i D\Sigma_x D^T\phi_i^T$, and $\sigma_{u_i}^2 = \phi_i L(\Sigma_x - \Sigma_e)L^T\phi_i^T$ where $\Sigma_e \geq 0$ is from Eq. 16 and $\Sigma_x \geq 0$ now must satisfy

$$A\Sigma_x + \Sigma_x A^T + BL(\Sigma_x - \Sigma_e) + (\Sigma_x - \Sigma_e)L^T B^T + GS_wG^T = 0 \qquad (18)$$

The simultaneous sensor and actuator selection problem may be formulated as

$$\min_{\substack{\alpha_i\in\{0,1\},\beta_i\in\{0,1\},\\ \Sigma_x\geq 0,\Sigma_e\geq 0,L}} \sum_{i=1}^{n_u} c_i^{(u)}\alpha_i + \sum_{i=1}^{n_y} c_i^{(y)}\beta_i$$
$$s.t. \quad \phi_i D\Sigma_x D^T\phi_i^T < \bar{z}_i^2, \quad i=1,\ldots,n_z$$
$$\phi_i L(\Sigma_x - \Sigma_e)L^T\phi_i^T < \alpha_i\bar{u}_i^2, i=1,\ldots,n_u$$
$$S_v^{-1} = \text{diag}\{\beta_i/\bar{\sigma}_{v_i}^2\}$$
$$A\Sigma_x + \Sigma_x A^T + BL(\Sigma_x - \Sigma_e) + (\Sigma_x - \Sigma_e)L^T B^T + GS_wG^T = 0$$
$$A\Sigma_e + \Sigma_e A^T + GS_wG^T - \Sigma_e C^T S_v^{-1} C\Sigma_e = 0 \qquad (19)$$

The MINLP of Eq. 19 can be converted to the following MICP (see Peng and Chmielewski[12] for details).

$$\min_{\substack{\alpha_i\in\{0,1\},\beta_i\in\{0,1\},\\ X>0,W>0,Y}} \quad \sum_{i=1}^{n_u} c_i^{(u)}\alpha_i + \sum_{i=1}^{n_y} c_i^{(y)}\beta_i$$
$$s.t. \quad \phi_i DXD^T\phi_i^T < \bar{z}_i^2, \quad i=1,\ldots,n_z$$
$$S_v^{-1} = \text{diag}\{\beta_i/\bar{\sigma}_{v_i}^2\}, \quad i=1,\ldots,n_y$$
$$\begin{bmatrix} \alpha_i\bar{u}_i^2 & \phi_i Y & 0 \\ Y^T\phi_i^T & X & I \\ 0 & I & W \end{bmatrix} > 0, \quad i=1,\ldots,n_u$$
$$(AX+BY)+(AX+BY)^T + GS_wG^T < 0$$
$$\begin{bmatrix} C^T S_v^{-1} C - A^T W - WA & WG \\ G^T W & S_w^{-1} \end{bmatrix} > 0 \qquad (20)$$

If α_i*, β_i*, X*, W*, and Y* denote the solution to Eq. 20, then a feasible controller under the sensor and actuator configuration α_i*, β_i* can be obtained as $L = Y^*(X^* - (W^*)^{-1})^{-1}$. As indicated in Peng and Chmielewski[12] additional variations of the hardware selection problem may be defined (mostly notably the PSI actuator selection problem and the closed-loop sensor selection problem). However, each is a special case of the simultaneous sensor and actuator selection problem.

Tubular Reactor Example

Consider a nonadiabatic tubular reactor of length L and radius R in which an elementary, irreversible, exothermic, and liquid phase reaction $A \rightarrow B$ takes place. Diffusion of heat and mass (coefficients k and D) are considered in the axial direction but are ignored in the radial. The reactant A enters with concentration $\bar{c}_{\text{in}}$ and temperature $\bar{T}_{\text{in}}$ and travels with a velocity v throughout the reactor length. The reactor is cooled by a jacket (transfer coefficient h) in which the coolant is maintained at a constant temperature T_w. Under these assumption, the dimensionless balance equations for mass and energy are (see Kumar and Seinfeld[23] for additional details).

$$\frac{\partial\xi'}{\partial t} = \frac{\partial^2\xi'}{\partial s^2} - Pe_m\frac{\partial\xi'}{\partial s} - k_1 r(\xi',\eta') \qquad (21)$$

$$\frac{\partial\eta'}{\partial t} = \frac{1}{Le}\frac{\partial^2\eta'}{\partial s^2} - Pe_h\frac{\partial\eta'}{\partial s} + k_1k_2 r(\xi',\eta') + k_3(\eta_w - \eta') \qquad (22)$$

where $\xi' = c/\bar{c}_{\text{in}}$, $\eta' = T/\bar{T}_{\text{in}}$, $s = l/L$, $t = \tau D/L^2$, $Pe_m = Lv/D$, $Pe_h = \rho v C_p L/k$, $Le = Pe_h/Pe_m$, $k_1 = L^2 k_0 e^{-k_4}/D$, $k_2 = (-\Delta H)\bar{c}_{\text{in}}/\rho C_p\bar{T}_{\text{in}}$, $k_3 = 2\bar{h}L^2/\rho C_p DR$, $k_4 = \bar{E}_A/R_g\bar{T}_{\text{in}}$,

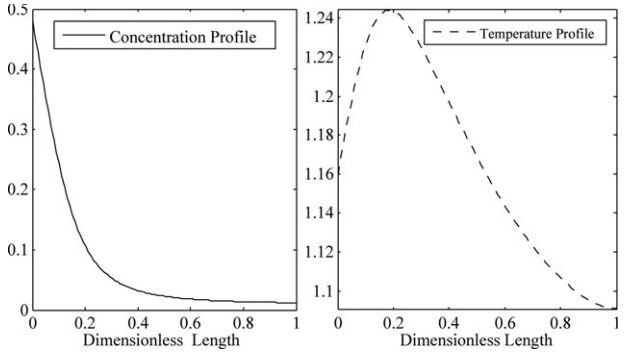

Figure 1. Steady-state concentration and temperature profiles.

$\eta_w = T_w/\bar{T}_{\text{in}}$, and $r(\xi', \eta') = \xi' \exp[k_4(1 - 1/\eta')]$. The boundary conditions are $\frac{\partial \xi'}{\partial s} = Pe_m(\xi' - 1)$ and $\frac{\partial \eta'}{\partial s} = Pe_h(\eta' - 1)$ at $s = 0$ and $\frac{\partial \xi'}{\partial s} = 0$ and $\frac{\partial \eta'}{\partial s} = 0$ at $s = 1$. As in the example of Kumar and Seinfeld,[23] the following parameter values are used $P = Pe_m = Pe_h = 5$, $k_1 = 0.875$, $k_2 = 0.5$, $k_3 = 13.0$, $k_4 = 25$, and $\eta_w = 1$. The resulting steady-state concentration and temperature profiles ($\bar{\eta}'(s)$ and $\bar{\xi}'(s)$) are shown in Figure 1.

Variation in the inlet concentration is assumed to be a disturbance. Although this will result in nonhomogeneous boundary conditions, they can be considered in a homogeneous way by simply adding $\delta(s)\xi_{\text{in}}{}'$ to Eq. 21, where $\xi'_{\text{in}} = c_{\text{in}}/\bar{c}_{\text{in}}$ (see Ray[31] for details). Variation in the dimensionless activation energy, k_4, is also assumed to be a disturbance. As for manipulated inputs, we assume the availability of two types. The first is the ability to change the reactor inlet temperature, resulting in the addition of $\delta(s)\eta_{\text{in}}{}'$ to Eq. 22, where $\eta'_{\text{in}} = T_{\text{in}}/\bar{T}_{\text{in}}$. In addition, we assume the ability to change the dimensionless heat-transfer coefficient, k_3, at various points along the reactor.

Remark: *On-line changes to the overall heat-transfer coefficient or available transfer area can be achieved by numerous mechanisms (for example, mechanical movement of insulating material or fin orientation). However, under the scenario of a constant temperature cooling jacket (which suggests phase change in the jacket fluid), such changes will have little impact on the transfer rate. A more realistic scenario would assume no phase change, which would require, at the very least, a model with axial temperature dependence within the cooling fluid (and most likely within the solid material of the transfer wall). While application of the proposed method on such a system is straightforward, the simpler (albeit less realistic) system is sufficient for illustrative purposes.*

On linearization around the steady-state profiles $\bar{\xi}'(s)$ and $\bar{\eta}'(s)$ one arrives at the following linear PDE system.

$$\frac{\partial \xi}{\partial t} = \frac{\partial^2 \xi}{\partial s^2} - P\frac{\partial \xi}{\partial s} + \mathcal{A}_{11}\xi + \mathcal{A}_{12}\eta + \mathcal{B}_1\mu + \mathcal{G}_1\omega \tag{23}$$

$$\frac{\partial \eta}{\partial t} = \frac{\partial^2 \eta}{\partial s^2} - P\frac{\partial \eta}{\partial s} + \mathcal{A}_{21}\xi + \mathcal{A}_{22}\eta + \mathcal{B}_2\mu + \mathcal{G}_2\omega \tag{24}$$

with boundary conditions $\frac{\partial \xi}{\partial s} = P\xi$ and $\frac{\partial \eta}{\partial s} = P\eta$ at $s = 0$ and $\frac{\partial \xi}{\partial s} = 0$ and $\frac{\partial \eta}{\partial s} = 0$ at $s = 1$, where $\xi = \bar{\xi}'(s,t) - \bar{\xi}'(s)$, $\eta = \eta'(s,t) - \bar{\eta}'(s)$, $\mathcal{A}_{11} = -k_1\bar{r}_\xi(s)$, $\mathcal{A}_{12} = -k_1\bar{r}_\eta(s)$, $\mathcal{A}_{21} = k_1k_2\bar{r}_\xi(s)$, $\mathcal{A}_{22} = k_1k_2\bar{r}_\eta(s) - k_3$, $\bar{r}_\xi(s) = \left.\frac{\partial r(\xi,\eta)}{\partial \xi}\right|_{\bar{\xi}',\bar{\eta}'}$ $\bar{r}_\eta(s) = \left.\frac{\partial r(\xi,\eta)}{\partial \eta}\right|_{\bar{\xi}',\bar{\eta}'}$,

$$\mathcal{B}_1 = [0\ 0]$$
$$\mathcal{B}_2 = [\delta(s)\ \bar{\eta}(s)]$$
$$\mu = [\eta_{in}\ k_3(s)]^T$$

where $\eta_{\text{in}} = \eta_{\text{in}}{}' - 1$.

$$\mathcal{G}_1 = [\delta(s) - k_1 r(\bar{\xi}', \bar{\eta}')(1 - 1/\bar{\eta}')]$$
$$\mathcal{G}_2 = [0\ k_1k_2 r(\bar{\xi}', \bar{\eta}')(1 - 1/\bar{\eta}')]$$
$$\omega = [\xi_{\text{in}}\ k_4]^T$$

where $\xi_{\text{in}} = \xi_{\text{in}}{}' - 1$. The eigenvalue problem: $\mathcal{L}_s\rho = \lambda\rho$ (where $\mathcal{L}_s = \frac{\partial^2}{\partial s^2} - P\frac{\partial}{\partial s}$ and $\frac{\partial \rho}{\partial s} = P\rho$ at $s = 0$ has the following solution, Ray[31]

$$\lambda_j = -(a_j^2 + P^2/4), \quad j = 1, \ldots, \infty \tag{25}$$

$$\rho_j(s) = H_j e^{Ps/2}\left(\cos(a_j s) + \frac{P}{2a_j}\sin(a_j s)\right), \quad j = 1, \ldots, \infty \tag{26}$$

where λ_j, ρ_j are the eigenvalues and eigenfunctions, respectively. If the inner product is defined as $\langle \rho_i, \rho_j \rangle = \int_0^1 e^{-Ps}\rho_i(s)\rho_j(s)ds$ and the boundary condition $\frac{\partial \rho}{\partial s} = 0$ at $s = 1$ is enforced then one finds that ρ_i will be an orthonormal sequence if a_j and H_j satisfy

$$\tan(a_j) = \frac{Pa_j}{a_j^2 - (P/2)^2}, \quad j = 1, \ldots, \infty \tag{27}$$

$$H_j = \left\{\int_0^1 \left(\cos(a_j s) + \frac{P}{2a_j}\sin(a_j s)\right)^2 ds\right\}^{-1/2}, \ j = 1, \ldots, \infty \tag{28}$$

Next define

$$\xi^{(N)}(s,t) = \sum_{i=1}^{N} x_i^{(\xi)}(t)\rho_i(s) \tag{29}$$

$$\eta^{(N)}(s,t) = \sum_{i=1}^{N} x_i^{(\eta)}(t)\rho_i(s) \tag{30}$$

where $x_i^{(\xi)}(t)$ and $x_i^{(\eta)}(t)$ are determined from $\frac{dx}{dt} = Ax + Bu + Gw$ where $x = [x^{(\xi)^T}\ x^{(\eta)^T}]^T$, $x^{(\xi)} = [x_1^{(\xi)}\ x_2^{(\xi)}, \ldots, x_N^{(\xi)}]^T$ and $x^{(\eta)} = [x_1^{(\eta)}\ x_2^{(\eta)}, \ldots, x_N^{(\eta)}]^T$. In this case,

$$A = \begin{bmatrix} A_{11} & A_{12} \\ A_{21} & A_{22} \end{bmatrix} \tag{31}$$

where the elements of A_{11} are $a_{ij}^{11} = \lambda_i\delta_{ij} - \langle \rho_j, k_1\bar{r}_\xi\rho_i \rangle$, A_{12} are $a_{ij}^{12} = -\langle \rho_j, k_1\bar{r}_\eta\rho_i \rangle$, A_{21} are $a_{ij}^{21} = \langle \rho_j, k_1k_2\bar{r}_\xi\rho_i \rangle$, and A_{22} are $a_{ij}^{22} = \lambda_i\delta_{ij} + \langle \rho_j, (k_1k_2\bar{r}_\eta - k_3)\rho_i \rangle$.

The vector of manipulated variables is $u = [u_o(t)u_1(t), \ldots, u_{n_u-1}(t)]^T$ where $u_o(t)$ changes the reactor feed temperature and $u_1(t), \ldots, u_{n_u-1}(t)$ change the heat-transfer coefficient at various locations along the length of the reactor. In this case

$$B = \begin{bmatrix} B_{11} & B_{12} \\ B_{21} & B_{22} \end{bmatrix}$$

where $B_{11} = 0$ and $B_{12} = 0$. The elements of B_{21} and B_{22} are $b_{i1}{}^{21} = \rho_i(0)$ and $b_{ij}^{22} = \langle \rho_i, \bar{\eta}' g_j^{(u)} \rangle$. Assuming the heat-transfer

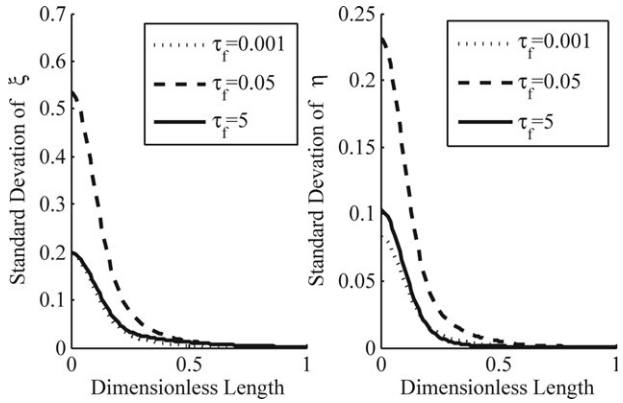

Figure 2. Standard deviation profiles with shaping filters.

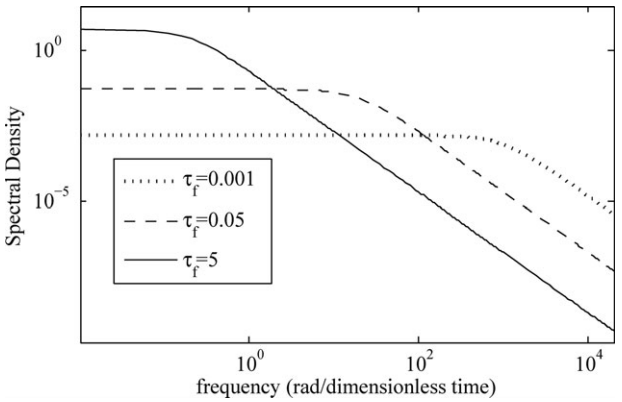

Figure 4. Power spectral densities of disturbance inputs.

coefficient can change only over a finite region of the reactor area, the corresponding actuators will take the following form

$$g_i^{(u)}(s) = \left\{ \begin{array}{ll} 1 & \text{if } s_i^{(\text{low})} \le s \le s_i^{(\text{hi})} \\ 0 & \text{otherwise} \end{array} \right\}$$

where $s_i^{(\text{hi})} \le s_{i+1}^{(\text{low})}$ is assumed. Thus, the elements of B_{22} become

$$b_{ij}^{22} = \int_{s_j^{(\text{low})}}^{s_j^{(\text{hi})}} e^{-Ps} \rho_i(s) \bar{\eta}'(s) ds$$

The disturbance vector is $w = [w_1(t)\ w_2(t)]^T$, where $w_1(t)$ and $w_2(t)$ represent changes in feed composition and activation energy, respectively. In this case

$$G = \begin{bmatrix} G_{11} & G_{12} \\ G_{21} & G_{22} \end{bmatrix}$$

where the elements of G_{11}, G_{12}, G_{21}, and G_{22} are $g_{i1}^{11} = \rho_i(0)$, $g_{i1}^{12} = \langle \rho_i, -k_1 r(\bar{\xi}', \bar{\eta}')(1 - 1/\bar{\eta}') \rangle$, $g_{i1}^{21} = 0$ and $g_{i1}^{22} = \langle \rho_i, k_1 k_2 r(\bar{\xi}', \bar{\eta}')(1 - 1/\bar{\eta}') \rangle$.

The set of available measurements is defined by $y = [y^{(\xi)T}\ y^{(\eta)T}]^T$ where $y^{(\xi)} = \left[y_1^{(\xi)}, \ldots, y_{n_{y\xi}}^{(\xi)} \right]$ and $y^{(\eta)} = \left[y_1^{(\eta)}, \ldots, y_{n_{y\eta}}^{(\eta)} \right]$. In this case

$$C = \begin{bmatrix} C_{11} & 0 \\ 0 & C_{22} \end{bmatrix} \tag{32}$$

Assuming the measurements of concentration and temperature are point-wise, the elements of C_{11} and C_{22} are $c_{ij}^{11} = e^{-Ps_i^{(y\xi)}} \rho_j(s_i^{(y\xi)})$ and $c_{ij}^{22} = e^{-Ps_i^{(y\eta)}} \rho_j(s_i^{(y\eta)})$ where $s_i^{(y\xi)}$ and $s_i^{(y\eta)}$ are the locations of each measurement. The performance output is defined as $z = [z^{(\xi)T}\ z^{(\eta)T}]^T$ where $z^{(\xi)} = \left[z_1^{(\xi)}, \ldots, z_{n_{z\xi}}^{(\xi)} \right]$ and $z^{(\eta)} = \left[z_1^{(\eta)}, \ldots, z_{n_{z\eta}}^{(\eta)} \right]$. In this case

$$D = \begin{bmatrix} D_{11} & 0 \\ 0 & D_{22} \end{bmatrix} \tag{33}$$

and the elements of D_{11} and D_{22} are $d_{ij}^{11} = e^{-Ps_i^{(z\xi)}} \rho_j(s_i^{(z\xi)})$ and $d_{ij}^{22} = e^{-Ps_i^{(z\eta)}} \rho_j(s_i^{(z\eta)})$ where $s_i^{(z\xi)}$ and $s_i^{(z\eta)}$ are the locations of interest.

Filtering of the Input Signals

In the above formulation of the tubular reactor model, the disturbance inputs are assumed to be white noise and the actuators are assumed to respond instantaneously. The following will illustrate the use of shaping filters to arrive at more realistic models. If the disturbance signal is the output of a first-order system $\tau_f \dot{x}_f = -x_f + w$ where x_f is the disturbance, τ_f is its correlation time, and w is Gaussian, zero mean, white noise with spectral density S_w, then the variance of x_f will be $\Sigma_f = S_w/2\tau_f$. For characterization purposes, assume the availability of off-line direct measurements of the disturbances. Using this measured data one can estimate the variance and correlation time of x_f (see Bendat and Piersol[35]). If these estimates are denoted $\hat{\Sigma}_f$ and $\hat{\tau}_f$, then our model of the disturbance, a shaping filter, should be defined as $\hat{\tau}_f \dot{x}_f = -x_f + w$ where the spectral density of w is set to $S_w = 2\hat{\tau}_f \hat{\Sigma}_f$. This particular form of the disturbance shaping filter allows one to easily analyze the impact of correlation

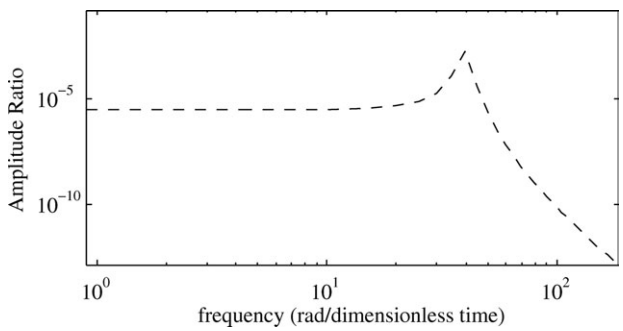

Figure 3. Bode diagram of reactor without shaping filter (input w_1 and output temperature at $s = 0.1$).

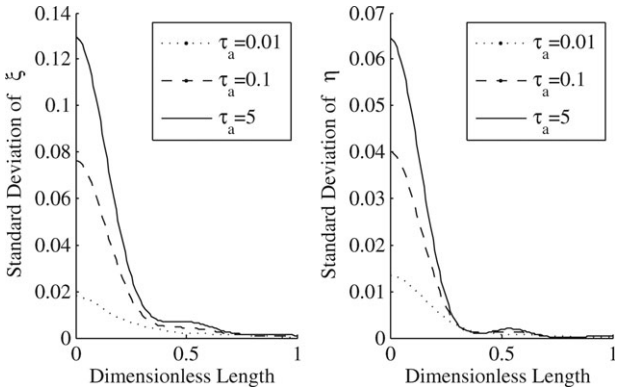

Figure 5. Standard deviation profiles with actuator response-time.

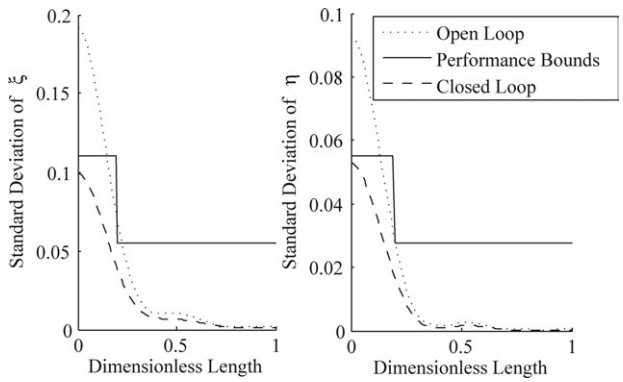

Figure 6. Standard deviation profiles for example 1 (performance bounds and closed-loop from case 1).

time on the output signals of the reactor. Consider the case of $w_2 = 0$ and $w_1 = x_f$ with $\hat{\Sigma}_f = 0.5$. Figure 2 shows the steady-state standard deviation profiles of the reactor for various values of $\hat{\tau}_f$. The case of $\tau_f = 0.001$ is nearly identical to that of the white noise case (at this point we drop the $\hat{}$ notation). When $\tau_f = 0.05$, the standard deviation profiles increase significantly. However, when τ_f is further increased (to 5) the standard deviation decreases. To understand why this peak near $\tau_f = 0.05$ occurs, begin by considering the Bode Diagram of the reactor without a shaping filter, depicted in Figure 3 (w_1 as the input and temperature at $s = 0.1$ as the output). The resonant frequency at 40 rad can be attributed to the two dominant eigenvalues of the A matrix of Eq. 31. Now consider the power spectral density plots of x_f with varying correlation times (Figure 4). These plots indicate the amount of power sent to the reactor as a function of frequency (when w_1 is set equal to x_f). It should be noted that the total power of each is the same, due to the fact that Σ_f was set to 0.5 for all cases. In the cases of $\tau_f = 5$, most of the power is in the low frequencies, and barely activates the resonant frequency of the reactor. In the $\tau_f = 0.001$ case, most of the power is moved to frequencies higher than the resonant but then is attenuated away by the reactor. The $\tau_f = 0.05$ case strikes balance by sending

Table 1. Performance Bounds and Solutions for Example 1

		$s < 0.2$	$s \geq 0.2$	Solution (s)	Minimum Cost
Case 1	$\bar{z}^{(\xi)}$	0.11	0.055	$\{u_o\}$	\$300
	$\bar{z}^{(\eta)}$	0.055	0.0275		
Case 2	$\bar{z}^{(\xi)}$	0.095	0.0475	$\{u_o, u_1\}$ $\{u_o, u_2\}$ $\{u_o, u_3\}$ $\{u_o, u_4\}$	\$550
	$\bar{z}^{(\eta)}$	0.0475	0.0238		
Case 3	$\bar{z}^{(\xi)}$	0.070	0.035	$\{u_o, u_1, u_2\}$ $\{u_o, u_1, u_3\}$ $\{u_o, u_1, u_4\}$ $\{u_o, u_1, u_5\}$ $\{u_o, u_2, u_3\}$ $\{u_o, u_2, u_4\}$ $\{u_o, u_2, u_5\}$	\$800
	$\bar{z}^{(\eta)}$	0.035	0.0175		
Case 4	$\bar{z}^{(\xi)}$	0.06	0.03	$\{u_o, u_1, u_2\}$ $\{u_o, u_1, u_3\}$	\$800
	$\bar{z}^{(\eta)}$	0.03	0.015	$\{u_o, u_2, u_3\}$	

Table 2. Solutions for Example 2

τ_a	Solution (s)	Minimum Cost
0.01	$\{u_o\}$	\$300
0.1	$\{u_o, u_1\}$	\$550
	$\{u_o, u_2\}$	
1.0	$\{u_1, u_2, u_3\}$	\$750
	$\{u_1, u_2, u_4\}$	

enough power to the high frequencies to activate the resonant frequency, but not so much that it gets attenuated away. The primary conclusion is that the frequency characteristics of the disturbances will have a large impact on plant performance and should be considered as an important part of process modeling.

To capture the response-time of the actuators it will be assumed that a command u must pass through a first-order filter, $\tau_a \dot{\boldsymbol{x}}_a = -\boldsymbol{x}_a + \boldsymbol{u}$, before impacting the process. Consider the $\tau_f = 0.05$ and $\Sigma_f = 0.5$ case of the previous paragraph and assume $u_o = x_a$ and $u_i = 0$, $i = 1, \ldots, n_u - 1$. If a FSI linear quadratic regulator is applied (with $Q = I$ and $R = 1$), then the standard deviation profiles of Figure 5 will result. As τ_a is increased, the standard deviation profiles increase. At $\tau_a = 5$ the profiles are nearly identical to that of the open-loop case, indicating that the slow response-time of the actuator is enough to make it completely ineffective.

In the next section, it is assumed that both disturbances are shaped by a first-order filter with $\tau_{f1} = 0.2$ and $\Sigma_{f1} = 0.5$ and $\tau_{f2} = 1$ and $\Sigma_{f2} = 1.5$. In addition, the first actuator will be assumed to have a first-order response-time ($\tau_a = 0.01$) while the other actuators $u_1, \ldots, u_{n_u-1}$ will be assumed to respond instantaneously. To incorporate into the finite dimensional model, the previous A matrix should replaced with

$$A = \begin{bmatrix} A_{11} & A_{12} & G_{11} & G_{12} & B_{11} \\ A_{21} & A_{22} & G_{21} & G_{22} & B_{21} \\ 0 & 0 & -1/\tau_{f1} & 0 & 0 \\ 0 & 0 & 0 & -1/\tau_{f2} & 0 \\ 0 & 0 & 0 & 0 & -1/\tau_a \end{bmatrix} \tag{34}$$

Similarly, B and G should be replaced with

$$B = \begin{bmatrix} 0 & B_{12} \\ 0 & B_{22} \\ 0 & 0 \\ 0 & 0 \\ 1/\tau_a & 0 \end{bmatrix} G = \begin{bmatrix} 0 & 0 \\ 0 & 0 \\ 1/\tau_{f1} & 0 \\ 0 & 1/\tau_{f2} \\ 0 & 0 \end{bmatrix} \tag{35}$$

In addition, both C and D will receive three additional columns of zeros. Finally, recall that S_w should be set to

$$S_w = \begin{bmatrix} 2\tau_{f1}\Sigma_{f1} & 0 \\ 0 & 2\tau_{f2}\Sigma_{f2} \end{bmatrix} \tag{36}$$

Table 3. Sensor Parameters for Example 3

	Type	Cost	$\bar{\sigma}_{v_i}$
y_1	Concentration	\$50	0.01
y_2	Concentration	\$200	0.001
y_3	Temperature	\$15	0.01
y_4	Temperature	\$80	0.001

Table 4. Solutions for Example 3

	$\bar{e}_z$	Solutions (s)	Minimum Cost
Case 1	0.03	$\{y_4 @ s = 0.00\}$ $\{y_4 @ 0.05\}$ $\{y_4 @ 0.10\}$ $\{y_4 @ 0.15\}$	\$80
Case 2	0.02	$\{y_4 @ s = 0.0\}$	\$80
Case 3	0.01	$\{y_2 @ s = 0.05, y_4 @ s = 0.00, y_4 @ s = 0.05\}$ $\{y_2 @ s = 0.05, y_4 @ s = 0.00, y_4 @ s = 0.10\}$	\$360

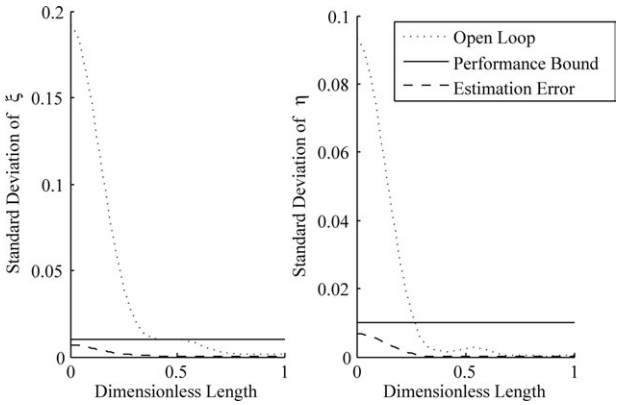

Figure 7. Estimation error standard deviation profiles for example 3 (performance bound and estimation error for case 3).

Case Studies

In this section, the three hardware selection problems will be illustrated using the tubular reactor example. All of the MICP problems of this section were solved using in-house developed branch-and-bound routines written in Matlab. The semidefinite programming subproblems called by these routines were solved by the "mincx" function provided in the Matlab robust control toolbox. All examples were solved on an Intel Pentium Dual CPU T300 at 2.00 GHz with 3.00 GB memory. In all cases, the performance outputs represent 100 evenly spaced locations along the length of the reactor, for a total of 200 output signals. In addition, five eigenfunctions were used in the spatial discretization step, resulting in a total of 10 state variables in the finite-dimensional model. A rerunning of the examples with 20 eigenfunctions gave identical solutions. A summary of problem size and computational effort for all four examples is given in Table 6.

Example 1. We begin with the actuator selection MICP of Eq. 13. The cost of actuator zero (inlet temperature) is \$300 with a maximum standard deviation $\bar{u}_o = 0.1$. The location for the remaining actuators (the heat transfer manipulations) is defined as: $s_1^{(\text{low})} = 0$, $s_1^{(\text{hi})} = s_2^{(\text{low})} = 0.1$, $s_2^{(\text{hi})} = s_3^{(\text{low})} = 0.2$, $s_3^{(\text{hi})} = s_4^{(\text{low})} = 0.3$, $s_4^{(\text{hi})} = s_5^{(\text{low})} = 0.4$, $s_5^{(\text{hi})} = s_6^{(\text{low})} = 0.5$, $s_6^{(\text{hi})} = 0.6$. Each of these six actuators has a cost of \$250 and a maximum standard deviation of 0.3 ($\bar{u}_i = 0.3$ i = 1,…,6). The open-loop standard deviation profiles along with the performance bounds for the first case of the example are depicted in Figure 6. The performance bounds for all four cases of this example are given in Table 1.

The solution to case 1 is to simply purchase actuator zero (manipulation of the inlet temperature). The three remaining cases illustrate the impact of tightening the performance bounds (all other parameters are unchanged). In case 2, it is observed that actuator zero is no longer enough to meet the performance requirement. As such four optimal solutions result, each using actuator zero and one other. It is interesting to note that u_o, u_5 and u_o, u_6 are not feasible for this case. In case 3, a similar situation arises, but this time three actuators are required. In case 4, the optimal cost is the same as case 3, but the set of optimal solutions is smaller.

The closed-loop performance using the actuator of case 1 and a feasible controller is also depicted in Figure 6. The closed-loop performance of all other cases resulted in similar plots. It is interesting to note that in case 1 the active constraint appears to be on the temperature profile at $s = 0$. It is presumed that an imposition of only this constraint would have resulted in identical solutions. However, this observation would have been impossible before obtaining the solution. For example, the constraint at $s = 0.2$ on the concentration profile could have also been active, if a slightly

Table 5. Performance Bounds and Solutions for Example 4

		$s < 0.2$	$s \geq 0.2$	Solution (s)	Minimum Cost
Case 1	$\bar{z}^{(\xi)}$	0.011	0.055	$\{u_o, u_1, y_4 @ s = 0.0\}$	\$630
	$\bar{z}^{(\eta)}$	0.055	0.0275	$\{u_o, u_1, y_4 @ s = 0.05\}$ $\{u_o, u_1, y_4 @ s = 0.10\}$ $\{u_o, u_1, y_4 @ s = 0.15\}$ $\{u_o, u_2, y_4 @ s = 0.0\}$ $\{u_o, u_2, y_4 @ s = 0.05\}$ $\{u_o, u_2, y_4 @ s = 0.10\}$ $\{u_o, u_2, y_4 @ s = 0.15\}$ $\{u_o, u_3, y_4 @ s = 0.0\}$ $\{u_o, u_3, y_4 @ s = 0.05\}$ $\{u_o, u_3, y_4 @ s = 0.10\}$	
Case 2	$\bar{z}^{(\xi)}$	0.095	0.0475	$\{u_0, u_1, y_4 @ s = 0.0\}$	\$630
	$\bar{z}^{(\eta)}$	0.0475	0.0238	$\{u_0, u_1, y_4 @ s = 0.05\}$	
Case 3	$\bar{z}^{(\xi)}$	0.070	0.035	$\{u_0, u_1, u_2, y_4 @ s = 0.0, 0.05, 0.1\}$	\$1,040
	$\bar{z}^{(\eta)}$	0.035	0.0175	$\{u_0, u_1, u_2, y_4 @ s = 0.0, 0.05, 0.15\}$	
Case 4	$\bar{z}^{(\xi)}$	0.06	0.03	$\{u_0, u_1, u_2, u_3, y_4 @ s = 0.0, 0.05\}$	\$1,210
	$\bar{z}^{(\eta)}$	0.03	0.015		

Table 6. Summary of Problem Size and Computational Effort

Problem	Number of Linear Matrix Inequality Variables	Solution Time (s)	Number of Iterations
Example 1; case 1	175	48	2
Example 1; case 2	175	158	11
Example 1; case 3	175	220	16
Example 1; case 4	175	285	12
Example 2; case 1	175	47	2
Example 2; case 2	175	127	9
Example 2; case 3	175	222	20
Example 3; case 1	111	1737	20
Example 3; case 2	111	1543	20
Example 3; case 3	111	364	2
Example 4; case 1	286	5193	1264
Example 4; case 2	286	123,510	1393
Example 4; case 3	286	108,880	1228
Example 4; case 4	286	50,006	564

different case set-up was considered. These observations along with the four cases of this example illustrate the importance of selecting performance bounds and their impact on the obtained solutions.

Example 2. In this example, the impact of changing the time-constant, τ_a, of actuator zero is illustrated. Assume all parameters are identical to case 1 of Example 1. If τ_a is changed from 0.01 to 0.1 (essentially slowing the response time of actuator zero), then it will require the assistance of u_1 or u_2 to meet the performance requirements (see Table 2). If $\tau_a = 1.0$, then actuator zero becomes so slow that it is not even included in the optimal solution.

Example 3. We now turn to the sensor selection MICP of Eq. 17. Regarding concentration sensors, two types are available, one with low precision and one with high precision, denoted y_1 and y_2. Similarly, two temperature sensing types are available, one with low precision and one with high precision, denoted y_3 and y_4. Table 3 lists the cost and noise spectral density for each. At each location any of the follow four sensors may be placed. The set of available locations is $s = 0.0$, 0.05, 0.1, 0.15, and 0.2.

Concerning the performance specification, the same estimation error standard deviation is required for all 200 outputs; the values used for the cases of the example are given in Table 4. In case 1, four optimal solutions are available, all using the high precision temperature sensor, y_4, but at different locations. Case 2 tightens the performance specification and results in only one of the four solutions from case 1. If the specification is tightened further, case 3, then the optimal solution requires three sensors, one concentration and two temperature. Figure 7, illustrates the relationship between performance bound and the resulting estimation error.

Example 4. We finally turn to the simultaneous sensor and actuator selection MICP of Eq. 20. The cases of Table 5 are identical to those of Example 1, with the exception of assuming a PSI structure. The set of available sensors is identical to Example 3. While resulting actuator selections show trends similar to Example 1, in general the number of selected actuators is increased. It is also noted that the only sensor selected in all cases is the high precision temperature sensor. It is presumed that a significant reduction in sensor cost parameters would result in the selection of many sensors, to the point of gathering information at levels similar to the FSI case. Under such a scenario one would expect the actuator selections to be very close to Example 1. However, this scenario of extremely low cost sensors is expected to be atypical. Thus, the primary benefit of the simultaneous selection problem is that it will determine the appropriate balance between sensor and actuator cost.

Conclusions

It has been shown that the minimum cost sensor and actuator selection methods of Peng and Chmielewski[12] can be applied to the distributed parameter systems. The illustrated methodology is to apply a spatial discritization method, such as the Galerkin approximation, to a linearized version of the infinite dimensional plant. The resulting finite dimensional model can then be readily applied to the hardware selection procedures. The importance of component dynamics and disturbance modeling was also highlighted.

Acknowledgments

The authors acknowledge financial support from the National Science Foundation (CBET - 0967906), the Department of Chemical and Biological Engineering, and the Armour College of Engineering at the Illinois Institute of Technology.

Literature Cited

1. Johnson CD. Optimization of a certain quality of complete controllability and observability for linear dynamic system. *J Basic Eng, ASME Trans*. 1969;91:228–238.
2. Muller PC, Weber HI. Analysis and optimization of certain qualities of controllability and observability for linear dynamical systems. *Automatica*. 1972;8:237–246.
3. Mellefont D, Sargent R. Selection of measurements for optimal feedback control. *Ind Eng Chem Process Des Dev*. 1978;17:549.
4. Morari M, Stephanopoulos G. Optimal selection of secondary measurements within the framework of state estimation in the presence of persistent unknown disturbances. *AIChE J*. 1980;26:247.
5. Romagnoli J, Alvarez J, Stephanopolus G. Variable measurement structures for process control. *Int J Control*. 1981;33:269.
6. Bagajewicz MJ. Design and retrofit of sensor networks in process plants. *AIChE J*. 1997;43:2300.
7. Chmielewski DJ, Palmer T, Manousiouthakis V. On the theory of optimal sensor placement. *AIChE J*. 2002;48:1001–1012.
8. Muske KR, Georgakis C. A methodology for optimal sensor selection in chemical processes. In: Proceedings of the American Control Conference, Anchorage, AK, 2002:4274–4278.
9. Alonso AA, Kevrekidis IG, Banga JR, Frouzakis CE. Optimal sensor location and reduced order observer design for distributed process systems. *Comput Chem Eng*. 2004;28:27–35.
10. Singh AK, Hahn J. Sensor location for stable nonlinear dynamic systems: multiple sensor case. *Ind Eng Chem Res*. 2006;45:3615–3623.
11. Peng JK, Chmielewski DJ. Optimal sensor network design using the minimally backed-off operating point notion of profit. In: Proceedings of the American Control Conference, 2005:220–224.
12. Peng JK, Chmielewski DJ. Covariance based hardware selection-part II: equivalence results for the sensor, actuator and simultaneous selection problems. *IEEE Trans Control Syst Technol* 2006;14:362–368.
13. Morari M, Stephanopoulos G, Arkun Y. Studies in the synthesis of control structures for chemical processes, part I: promulgation of the problem. Process decomposition and the classification of the control task. Analysis of the optimizing control structures. *AIChE J*. 1980; 26:220–232.
14. Hovd M, Skogestad S. Procedure for regulatory control structure selection with application to the FCC process. *AIChE J*. 1993;39: 1938–1953.
15. Narraway L, Perkins J. Selection of process control structure based on economics. *Comput Chem Eng*. 1994;18:511–515.

16. Lee JH, Braatz RD, Morari M, Packard A. Screening tools for robust control structure selection. *Automatica*. 1995;31:229–235.
17. Loeblein C, Perkins J. Economic analysis of different structures of on-line process optimization systems. *Comput Chem Eng*. 1996;20: S551–S556.
18. Cao Y, Rossiter D. An input pre-screening technique for control structure selection. *Comput Chem Eng*. 1997;21:563–569.
19. Wisnewski PA, Doyle FJ. Control structure selection and model predictive control of the Weyerhaeuser digester problem. *J Process Control*. 1998;8:487–495.
20. Heath JA, Kookos IK, Perkins JD. Process control structure selection based on economics. *AIChE J*. 2000;46:1998–2016.
21. van de Wal M, de Jager B. Review of methods for input/output selection. *Automatica*. 2001;37:487–510.
22. Yu TK, Seinfeld JH. Observability and optimal measurement location in linear distributed parameter systems. *Int J Control*. 1973; 18:785–799.
23. Kumar S, Seinfeld JH. Optimal location of measurements in tubular reactors. *Chem Eng Sci*. 1978;33:1507–1516.
24. Harris TJ, Macgregor JF, Wright JD. Optimal sensor location with an application to a packed bed tubular reactor. *AIChE J*. 1980; 26:910–916.
25. Morari M, O'Dowd MJ. Optimal sensor location in the presence of nonstationary noise. *Automatica*. 1980;16(5):463–480.
26. Van de Wouwer A, Point N, Porteman S, Remy M. An approach to the selection of optimal sensor locations in distributed parameter systems. *J Process Control*. 2000;10:291.
27. Faulds AL, King BB. Sensor location in feedback control of partial differential equation systems. In: Proceedings of the IEEE International Conference Control Applications, 2000:536–541.
28. Antoniades C, Christofides PD. Integrating nonlinear output feedback control and optimal actuator/sensor placement for transport-reaction processes. *Chem Eng Sci*. 2001;56:4517–4535.
29. Armaou A, Demetriou MA. Optimal actuator/sensor placement for linear parabolic PDEs using spatial H2 norm. *Chem Eng Sci*. 2006; 61:7351–7367.
30. Kubrusly CS, Malebranche H. Sensors and controllers location in distributed systems—a survey. *Automatica*. 1985;21:117–128.
31. Ray WH. *Advanced Process Control*. New York: McGraw-Hill, 1981.
32. Fletcher CAJ. *Computational Galerkin Methods*. New York: Springer-Verlag, 1984.
33. Christofides PD, Daoutidis P. Nonlinear control of diffusion-convection-reaction processes. *Comput Chem Eng*. 1996;20 (Suppl 2): S1071–S1076.
34. Chmielewski DJ, Peng JK. Covariance based hardware selection-Part I: globally optimal actuator selection. *IEEE Trans Control Syst Technol*. 2006;14:355–361.
35. Bendat JS, Piersol AG. *Random Data: Analysis and Measurement Procedures. A Wiley-Interscience publication*. New York: Wiley, 1990.

Manuscript received Feb. 9, 2011, revision received July 20, 2011, and final revision received Sept. 21, 2011.